

INTERSTELLAR COMMUNICATION. VI. SEARCHING X-RAY SPECTRA FOR NARROWBAND COMMUNICATION

MICHAEL HIPPKÉ¹ AND DUNCAN H. FORGAN^{2,3}¹*Sonneberg Observatory, Sternwartestr. 32, 96515 Sonneberg, Germany*²*SUPA, School of Physics & Astronomy, University of St Andrews, North Haugh, St Andrews, Scotland, KY16 9SS, UK*³*St Andrews Centre for Exoplanet Science, University of St Andrews, UK*

ABSTRACT

We have previously argued that targeted interstellar communication has a physical optimum at narrowband X-ray wavelengths $\lambda \approx 1$ nm, limited by the surface roughness of focusing devices at the atomic level (Hippke & Forgan 2017). We search 24,247 archival X-ray spectra (of 6,454 unique objects) for such features and present 19 sources with monochromatic signals. Close examination reveals that these are most likely of natural origin. The ratio of artificial to natural sources must be $\lesssim 0.01\%$. This first limit can be improved in future X-ray surveys.

1. INTRODUCTION

Our previous work found the optimal frequency for data rate maximizing interstellar communication, given advanced technology, to be limited by the surface roughness of focusing devices at the atomic level. Depending on the material used for the reflective coating, the optimal wavelength is $\lambda \approx 0.5\text{--}2$ nm ($E \approx$ keV) for distances out to kpc (Hippke & Forgan 2017). While this limit can be surpassed by beam-forming with electromagnetic fields (e.g. using a free electron laser), such methods are not energetically competitive. Current lasers are not yet cost efficient for nm wavelength, with a gap of two orders of magnitude, but future technological progress may converge on the physical optimum.

As detailed in Hippke & Forgan (2017), the ideal spectrum for a maximum data rate connection will have a hard cut at $\lambda > 0.5$ nm due to mirror surface roughness. Bandwidth depends on the trade-off between the number of modes and the beam angle width. More wavelengths encode more bits per photon, however longer wavelengths have larger angular spread. The encoding efficiency follows a logarithmic relation with the number of modes (Hippke 2017), so that the bandwidth will be small ($< 100\%$) in realistic cases. As nanosecond time slots give 10^9 modes per second, the monochromatic number of photons can be up to 10^8 s⁻¹ before the mode penalty exceeds 1% in bit rate. Consequently, a GB/s connection will be monochromatic if nanosecond technology is available. Such a connection over pc distances

can be achieved with aperture sizes $D_t = D_r = 10$ m at modest (MW) power.

Optimal communication will be tightly focused with beam angles at the optimum wavelength $\lambda \approx$ nm of $\theta = 0.2$ mas/ D_t (m) due to diffraction. Randomly intercepting such beams between a large ($n = 10,000$) club of communicating galactic civilizations is unlikely (Forgan 2014). Thus, we may only hope that such communication is directed at Earth.

Based on these assumptions, we may search the sky for narrowband or monochromatic sources between 0.5 and a few nm. A comparable search for optical laser signals in spectra was carried out by Tellis & Marcy (2017) with a null result for 5,600 FGKM stars. There are 5.7×10^7 X-ray sources visible to XMM-Newton over the entire sky (Cappelluti et al. 2007), and spectra have been taken for 24,247 (4×10^{-4} of the visible sources). Checking these spectra for artificial features can place a first upper bound to the number of optimally communicating (towards us) civilizations.

2. METHOD

X-rays can only be observed from space due to atmospheric absorption. Several current X-ray satellites cover the wavelengths of interest: Swift (0.2–10 keV, Burrows et al. 2005), Chandra (0.1–10 keV, Garmire et al. 2003) and XMM-Newton (0.1–12 keV, Jansen et al. 2001), while INTEGRAL is only sensitive to higher energies (3 keV–10 MeV), and its spectrometer only covers the region 20 keV – 8 MeV which is outside of our window of interest. Because of their designs with grazing incidence mirrors, all telescopes have small collecting areas (0.01 m², 0.04 m² and 0.45 m² for Swift, Chandra and XMM, respectively) (Gilli et al. 2007). With a spec-

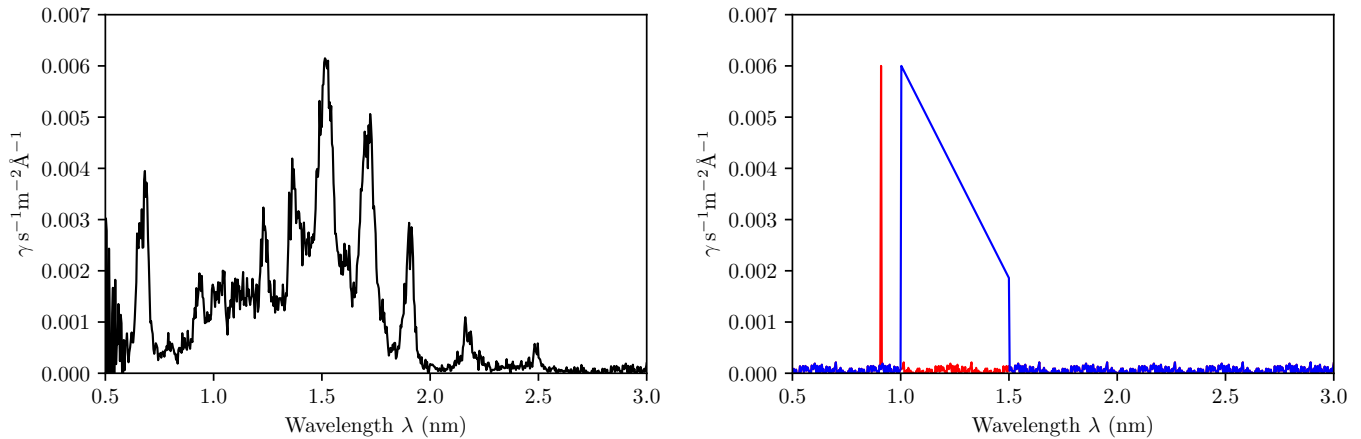


Figure 1. Left: X-ray spectrum taken with XMM-Newton for Kepler’s 1604 supernova remnant (Cassam-Chenaï et al. 2004). Right: Hypothetical spectra of monochromatic (red) and narrow (50% bandwidth, blue) X-ray signals.

tral resolution of $R = 800$ between 0.35–2.5 keV (3.5 eV at 1 keV energy), XMM is well equipped for the proposed narrow-band X-ray signals (den Herder et al. 2001).

As an example, we show the spectrum of Kepler’s supernova remnant (SN1604) as observed with XMM-Newton by Cassam-Chenaï et al. (2004) in Figure 1 (left panel). For comparison, synthetic monochromatic and narrow-band spectra are shown in the right panel.

2.1. Data

The latest generation of space-based X-ray telescopes offers high sensitivity, spatial resolution and energy range. Results demonstrate the potential of Galactic X-ray surveys to detect a wide variety of source types, such as coronally-active binaries (Hérent et al. 2006), evolved protostars and T Tauri stars (Feigelson & Montmerle 1999), or isolated neutron stars (Haberl & Pietsch 2007).

In this paper, we utilize observations drawn from the XMM-Newton public data archive. Specifically, we query the archive for all reduced, calibrated observations taken with the Reflection Grating Spectrometers which operate between 0.5 – 3.5 nm. This search yields a total of 24,247 spectra of 6,454 unique objects with exposure times between one second and 40 hours, and a mean (median) exposure time of 8.3 (5.8) hours. We download all spectra in FITS format using a custom-made script and create figures of each spectrum.

2.2. Feature search

The most prominent X-ray line emitting elements in the XMM-Newton passband are Iron, Oxygen, Magnesium, Sulfur, Silicon, Sodium, Calcium, Argon, Neon and Nickel (den Herder et al. 2001; Gu et al. 2016). Most, but not all emission lines appear spectrally resolved (e.g., Werner et al. 2006; Whewell et al. 2016). Consequently, it is possible that natural emission resembles a single monochromatic signal, in case only one such narrow line emitting element would be detectable above

the noise. We search for single peaks using a 1D wavelet (Du et al. 2006) with accepted peak widths of 1–2 bins ($\approx 3.5 - 7$ eV at keV), as implemented by SciPy, and requiring $\text{SNR} > 5$ for the highest peak, with no other peaks of $\text{SNR} > 4$ being present in the same spectra. This criteria is necessary because many spectra show tens to hundreds of emission lines of natural origin, and it is impossible to distinguish these from the artificial case.

For the narrowband feature search, we required the presence of a peak with a minimum width of two bins (≈ 7 eV at keV) at $\text{SNR} > 5$ and at least one sharp edge, i.e. a transition to $\text{SNR} < 3$ on one side of the peak. No additional peaks with $\text{SNR} > 4$ in the same spectrum were tolerated.

3. RESULTS

After the automatic search and visual examination, 19 spectra with a “potentially monochromatic” feature were identified (Table 1), and none with a narrow-band feature. To verify the correctness of the algorithm, we relaxed the SNR requirements and visually examined the best candidates. No spectra of interest were found.

A literature search for the 19 spectra with a “potentially monochromatic” feature shows that all of them are identical with natural, astrophysical sources, such as galaxies and variable stars. Spatially resolved sources, such as the Cygnus Loop supernova remnant, exhibit different spectral features in different regions (pointings), resulting in single peak detection if SNR is low. The same mechanism appears to be present as well for all other sources. We found no indication for anything artificial.

As an example, rho Oph (the “X-ray lighthouse”) shows strong and time-variable emissions between 0.5–3.5 nm, including FeXXIV, NeX, NeIX, OVIII, and CVI (Pillitteri et al. 2017).

A spectrum for HD189733 is shown in Figure 2, with a prominent peak at 1.89 nm, the oxygen emission line

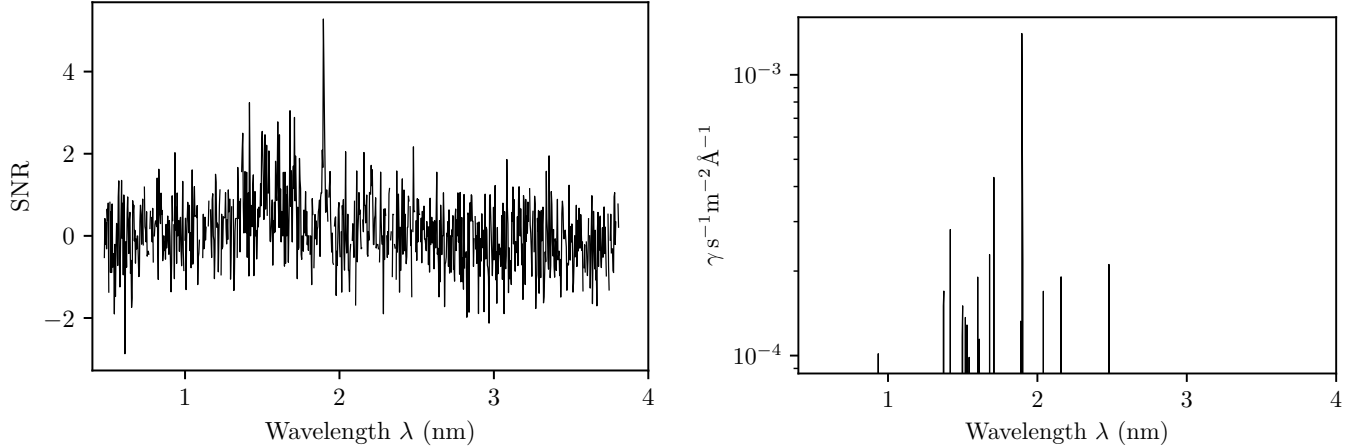


Figure 2. Left: Spectrum for HD189733 in units of SNR used for visual examination (XMM-Newton ID#0692290301). Only one peak with $\text{SNR} > 5$ is found. Right: The same spectrum in physical flux units. For clarity, only channels with $\text{SNR} > 2$ are shown.

OVIII Lyman- α (Walker et al. 1974; Pounds & Vaughan 2011). This is the most commonly found emission line, detected in 7 of the 19 spectra. A detailed discussion of the natural emission properties of these lines is beyond the scope of this paper.

4. DISCUSSION

We can calculate the expected SNR for a detector such as XMM-Newton for the case of optimal X-ray communication whose photon count scales as (Hippke & Forgan 2017)

$$\gamma \approx d^{-2} D_t^2 D_r^2 P_t (\text{s}^{-1}) \quad (1)$$

where the distance d is in pc, transmitter and receiver apertures D_t and D_r are in m and power P_t is in Watt. As an example, we use a $D_t = 1$ m telescope at Proxima Cen ($d = 1.3$ pc) with $P = 1$ W and XMM-Newton's quantum efficiency of 50% at keV energy (Strüder et al. 2001). The monochromatic photon count for XMM is then 0.3 s^{-1} , so that a high SNR detection with 100 photons in one spectral channel is achieved after 6 min.

If a survey spends 10 min on each source, a clear detection in this framework is possible if the transmitter power $P_t > 0.5 d^2 D_t^{-2}$.

As an example, for $D_t = 1$ m, P_t scales out to 50 W (5 kW, 500 kW) at distances of 10 pc (100 pc, kpc). Equally, for kW power the aperture D_t would need to

grow to 0.2 (2, 20 kW) for distances of 10 pc (100 pc, kpc).

These requirements are modest even for current technology, and it makes such communications technologically plausible. A survey with a duty cycle of 50% using XMM-Newton could observe 5×10^4 sources per year. If the target list are the nearest stars of stellar types M, K, G, the survey could probe all of these stars out to 40 (100 pc) within one (ten) years.

4.1. Upper limit on X-ray sources targeted at us

The archival sample contains mostly established astrophysical sources, such as supernova remnants and radio-loud stars and galaxies. Targeting obviously natural (and sometimes hostile) sources makes the detection of artificial signals less likely, and upper limits too conservative.

We detect no artificial signals in 6,454 unique objects, and therefore the ratio of artificial to natural sources must be $\lesssim 0.01\%$. This is not a strict limit, because the data does not come from a contiguous survey. An unbiased future spectral X-ray survey should target unlikely sources of powerful narrowband X-rays, such as nearby and field F, G, K, M stars.

5. CONCLUSION

Close examination of 24,247 archival X-ray spectra revealed 19 candidates with single monochromatic emission lines. All of these are found to be likely of natural origin. This first limit can be improved in future X-ray surveys.

APPENDIX

Table 1. Objects with monochromatic X-ray signals

Object	Type	Peak λ (nm)	ID#	Comment
NGC 720	Galaxy	0.521	0112300101	Other peaks exist (Jeltema et al. 2003)
4C 29.30	Seyfert 2 galaxy	3.851	0504120101	Strong GHz source (Jamrozny et al. 2007)
Cygnus Loop	Supernova remnant	3.426	0018140101	Extended source (Levenson et al. 1997)
zet CMa	Cepheid variable	1.899	0600530101	Pulsating magnetosphere (Shultz et al. 2017)
HD 189733	BY Dra type variable	1.896	0744981701	Hot Jupiter exoplanet (Bouchy et al. 2005)
eps Per	Beta Cep type variable	1.896	0761090801	Binary (Libich et al. 2006), pulsations (Saio et al. 2000)
Kappa Sco	Beta Cep type variable	2.162	0503500201	Binary, pulsations (Harmanec et al. 2004; Uytterhoeven et al. 2005)
56 Tau	Alpha2 CVn type variable	1.896	0201360201	Period 1.57 d (North & Adelman 1995)
HD 283572	T Tau-type variable	0.524	0101441001	SED peak at keV (Favata et al. 1998)
CE 315 (V396 Hya)	Nova, AM CVn binary	0.557	0302160201	Cataclysmic variable (Ramsay et al. 2006)
RBS 1955 (V405 Peg)	Dwarf nova	0.589	0604060101	Cataclysmic binary (Thorstensen et al. 2009)
61 Cyg A+B	Double star	1.899	0041740301	Nearby K5V+K7V (Robrade et al. 2012; Boro Saikia et al. 2016)
rho Oph	Double star	0.553	0305540601	“X-ray lighthouse” period 1.4 d (Pillitteri et al. 2017)
HD 54662	Double star	0.575	0780150101	Spectroscopic binary (Boyajian et al. 2007)
IGR J17091-3624	Low mass X-ray binary	0.560	0406140401	“Exotic variability” (Court et al. 2017)
HD 79555	High proper-motion star	1.896	0602830401	Young (35 Myr, Maldonado et al. 2010) binary (Mason et al. 2001)
CN Leo (Wolf 359)	Flare star	1.899	0200530701	3rd closest star (2.4 pc), dM6e (Wing & Ford 1969)
UV Ceti (GJ 65 B)	Flare star	0.474	0111430201	Nearby binary M5.5Ve+M6Ve (Kervella et al. 2016)
eta Car	Emission-line star	2.483	0560580201	Colliding-wind binary (Leser et al. 2017)

REFERENCES

- Boro Saikia, S., Jeffers, S. V., Morin, J., et al. 2016, *A&A*, 594, A29
- Bouchy, F., Udry, S., Mayor, M., et al. 2005, *A&A*, 444, L15
- Boyajian, T. S., Gies, D. R., Dunn, J. P., et al. 2007, *ApJ*, 664, 1121
- Burrows, D. N., Hill, J. E., Nousek, J. A., et al. 2005, *SSRv*, 120, 165
- Cappelluti, N., Hasinger, G., Brusa, M., et al. 2007, ArXiv e-prints, [arXiv:0704.2293](https://arxiv.org/abs/0704.2293)
- Cassam-Chenaï, G., Decourchelle, A., Ballet, J., et al. 2004, *A&A*, 414, 545
- Court, J. M. C., Altamirano, D., Pereyra, M., et al. 2017, *MNRAS*, 468, 4748
- den Herder, J. W., Brinkman, A. C., Kahn, S. M., et al. 2001, *A&A*, 365, L7
- Du, P., Kibbe, W. A., & Lin, S. M. 2006, *Bioinformatics*, 22, 2059
- Favata, F., Micela, G., & Sciortino, S. 1998, *A&A*, 337, 413
- Feigelson, E. D., & Montmerle, T. 1999, *ARA&A*, 37, 363
- Forgan, D. H. 2014, *Journal of the British Interplanetary Society*, 67, 232
- Garmire, G. P., Bautz, M. W., Ford, P. G., Nousek, J. A., & Ricker, Jr., G. R. 2003, in *Proc. SPIE, Vol. 4851, X-Ray and Gamma-Ray Telescopes and Instruments for Astronomy.*, ed. J. E. Truemper & H. D. Tananbaum, 28
- Gilli, R., Comastri, A., & Hasinger, G. 2007, *A&A*, 463, 79
- Gu, L., Mao, J., Costantini, E., & Kaastra, J. 2016, *A&A*, 594, A78
- Haberl, F., & Pietsch, W. 2007, *A&A*, 476, 317
- Harmanec, P., Uytterhoeven, K., & Aerts, C. 2004, *A&A*, 422, 1013
- Hérent, O., Motch, C., & Guillout, P. 2006, in *ESA Special Publication, Vol. 604, The X-ray Universe 2005*, ed. A. Wilson, 91
- Hippke, M. 2017, ArXiv e-prints, [arXiv:1712.05682](https://arxiv.org/abs/1712.05682) [[astro-ph.IM](https://arxiv.org/archive/astro-ph)]
- Hippke, M., & Forgan, D. H. 2017, ArXiv e-prints, [arXiv:1711.05761](https://arxiv.org/abs/1711.05761) [[astro-ph.IM](https://arxiv.org/archive/astro-ph)]
- Jamrozy, M., Konar, C., Saikia, D. J., et al. 2007, *MNRAS*, 378, 581
- Jansen, F., Lumb, D., Altieri, B., et al. 2001, *A&A*, 365, L1
- Jeltema, T. E., Canizares, C. R., Buote, D. A., & Garmire, G. P. 2003, *ApJ*, 585, 756
- Kervella, P., Mérand, A., Ledoux, C., Demory, B.-O., & Le Bouquin, J.-B. 2016, *A&A*, 593, A127
- Leser, E., Ohm, S., Fülling, M., et al. 2017, ArXiv e-prints, [arXiv:1708.01033](https://arxiv.org/abs/1708.01033) [[astro-ph.HE](https://arxiv.org/archive/astro-ph)]
- Levenson, N. A., Graham, J. R., Aschenbach, B., et al. 1997, *ApJ*, 484, 304
- Libich, J., Harmanec, P., Vondrák, J., et al. 2006, *A&A*, 446, 583
- Maldonado, J., Martínez-Arnáiz, R. M., Eiroa, C., Montes, D., & Montesinos, B. 2010, *A&A*, 521, A12
- Mason, B. D., Wycoff, G. L., Hartkopf, W. I., Douglass, G. G., & Worley, C. E. 2001, *AJ*, 122, 3466
- North, P., & Adelman, S. J. 1995, *A&AS*, 111, 41
- Pillitteri, I., Wolk, S. J., Reale, F., & Oskinova, L. 2017, *A&A*, 602, A92
- Pounds, K. A., & Vaughan, S. 2011, *MNRAS*, 413, 1251
- Ramsay, G., Groot, P. J., Marsh, T., et al. 2006, *A&A*, 457, 623
- Robrade, J., Schmitt, J. H. M. M., & Favata, F. 2012, *A&A*, 543, A84
- Saio, H., Kambe, E., & Lee, U. 2000, *ApJ*, 543, 359
- Shultz, M., Wade, G. A., Rivinius, T., et al. 2017, *MNRAS*, 471, 2286
- Strüder, L., Briel, U., Dennerl, K., et al. 2001, *A&A*, 365, L18
- Tellis, N. K., & Marcy, G. W. 2017, *AJ*, 153, 251
- Thorstensen, J. R., Schwarz, R., Schwöpe, A. D., et al. 2009, *PASP*, 121, 465
- Uytterhoeven, K., Briquet, M., Aerts, C., et al. 2005, *A&A*, 432, 955
- Walker, Jr., A. B. C., Rugge, H. R., & Weiss, K. 1974, *ApJ*, 192, 169
- Werner, N., de Plaa, J., Kaastra, J. S., et al. 2006, *A&A*, 449, 475
- Whewell, M., Branduardi-Raymont, G., & Page, M. J. 2016, *A&A*, 595, A85
- Wing, R. F., & Ford, Jr., W. K. 1969, *PASP*, 81, 527